

# Topographic and Reflectometric Investigation of Crystallographic Defects and Surface Roughness in 4H Silicon Carbide Homoepitaxial Layers Deposited at Various Growth Rates

W. WIERZCHOWSKI<sup>a</sup>, K. WIETESKA<sup>b</sup>, K. MAZUR<sup>a</sup>, K. KOŚCIEWICZ<sup>a</sup>, T. BALCER<sup>a</sup>,  
W. STRUPIŃSKI<sup>a</sup> AND C. PAULMANN<sup>c</sup>

<sup>a</sup>Institute of Electronic Materials Technology, Wólczyńska 133, 01-919 Warsaw, Poland

<sup>b</sup>National Centre for Nuclear Research, Andrzeja Sołtana 7, 05-400 Otwock-Świerk, Poland

<sup>c</sup>HASYLAB at DESY, Notkestr. 85, 22603 Hamburg, Germany

Undoped 4H silicon carbide epitaxial layers were deposited by means of CVD method with growth rates of 2  $\mu\text{m/h}$ , 5  $\mu\text{m/h}$  and 11  $\mu\text{m/h}$  at 1540 °C on *n*-doped 8°, 4° and 0° off-cut 4H-SiC (00·1) substrates. The structural defects were studied before and after growth of the epitaxial layers by means of conventional Lang topography, synchrotron white beam and monochromatic beam topography and by means of X-ray specular reflectometry. The topographic investigations confirmed the continuation of the dislocations in the epitaxial deposit on the 8° and 4° off-cut substrates without new extended defects. The important difference occurred in the surface roughness of the epitaxial layers, which increased for higher growth rates. The epitaxial layers grown on 0° off-cut substrates at analogous condition contained usually other SiC polytypes, but the influence of the growth rate on the distribution of the polytypes was observed.

PACS: 61.05.cm, 61.72.Ff, 61.72.up

## 1. Introduction

The silicon carbide technology of electronic and optoelectronic devices has been commercially developed in recent years, including a wide use of epitaxial techniques. The deposition of silicon carbide epitaxial layers is most commonly realized using chemical vapor deposition (CVD) method [1]. Unlike in the case of bulk crystals, where the growth of 6H polytype is the simplest, it is quite easy to grow epitaxial layers of 4H SiC polytype on 4H SiC substrates. To obtain the 3C SiC polytype, epitaxial technique on silicon substrates is commonly used [2].

An important factor conditioning the successful growth of 4H SiC homoepitaxial layers is the off-cut of the substrates from (00·1) planes. The most commonly applied off-cut value is 8°. The suggested “step-flow” growth mechanism [3, 4] consists in the deposition of crystallites along the edges of the steps formed on disoriented surface in the process of the initial chemical etching before the epitaxial process. During growth the edges of the steps continuously move along the surface. The use of substrate wafers with smaller off-cut is more difficult and usually requires some modification of the growth conditions. It is, however attractive in the view of reduction of material losses during the preparation of substrate wafers. One of the most important problems at the lower off-cut values is how to avoid so called “step bunching” consisting in formation the irregular steps (bunches

of steps) in the pre-etching process performed at a high temperature in the atmosphere of hydrogen mixed with propane.

The epitaxial growth on 4° off-cut substrates with the use of so called hot wall growth reactor had been recently described by Wada *et al.* [5] and by Chen and Capano [6]. The quality of the layers is also dependent on the chemical composition of the used precursors strongly affecting the growth rate. It had been analyzed by Kojima *et al.* [7], Myers *et al.* [8] and Fujiwara *et al.* [9]. The required effect of micro-pipes overgrowth is stimulated by a larger off-cut and higher growth rate. The growth of epitaxial films on differently oriented substrates had also been considered by Landini and Brandes [10] and by Nakamura *et al.* [11]. The specific “carrot-like” defects occurring in 4H epitaxial layers had been described by Benemara *et al.* [12]. The use of X-ray diffraction topography in studying of 4H SiC homoepitaxial layers had been included in papers by Tsuchida *et al.* [13], Zheng *et al.* [14] and by Huh *et al.* [15].

The growth of single polytype 4H-SiC homoepitaxial layer on 0° off-cut substrates is very difficult, because the “step-flow” mechanism is not possible. The successful growth of such layer was reported by Kościewicz *et al.* [16].

The technology of SiC bulk crystals and epitaxial layers is currently being developed in the Institute of Electronic Materials Technology (ITME) providing the opportunity

of wide use of X-ray methods of characterization exploring conventional and synchrotron sources of radiation. Some results of the growth of the epitaxial layers on the substrates with small off-cut obtained at ITME were published elsewhere [16], while some results on the influence of surface finishing on the perfection of 4H SiC homoepitaxial layers were published by Mazur *et al.* [17].

The purpose of the present paper was to study the structural defects and the surface roughness in 4H silicon carbide homoepitaxial layers grown on the substrates with the off-cut being smaller than the most frequently used  $8^\circ$  with different growth rate, which was one of the parameters suggested by many authors as the one to be altered at the lower off-cut [5,6]. Various values of the growth rate parameter were used, as suggested for the small off-cut case in refs. [5,6].

## 2. Experimental methods

The presently investigated 4H silicon carbide epitaxial layers were grown with CVD method with the use of Aixtron VP 508 equipment at hot wall regime and  $\text{CH}_4$  and  $\text{C}_3\text{H}_8$  precursors. The growth reactor is a horizontal one, but offers some additional possibilities (gas flow, additional sample motion).

The layers were not intentionally doped and were deposited on *n*-type 4H silicon carbide commercial substrates produced by Cree Incorporated with the concentration of nitrogen close to  $10^{17} \text{ cm}^{-3}$  and low concentration of defects.  $0^\circ$ ,  $4^\circ$  and  $8^\circ$  off-cut 4H-SiC ( $00 \cdot 1$ ) substrates were used. Three growth rates of  $2 \mu\text{m/h}$ ,  $5 \mu\text{m/h}$  and  $11 \mu\text{m/h}$  were applied for each off-cut – the middle value is most commonly used in the technological process. The thickness of the epitaxial deposit was close to  $5 \mu\text{m}$ . The main experiment included nine samples with the layers deposited on substrates with all three off-cut values at  $1540^\circ\text{C}$ . Some layers deposited on  $0^\circ$  off-cut 4H SiC substrates with a lower growth rate at higher temperature providing single polytype composition were also studied.

The samples were characterized with use of X-ray methods of characterization exploring conventional and synchrotron sources of radiation. A number of complementary methods of X-ray diffraction topography have been applied including conventional Lang transmission topography using  $\text{Mo K}\alpha_1$  radiation and synchrotron topography using white beam and monochromatic beam radiation. The white, and monochromatic beam synchrotron topographic investigations were performed respectively at the experimental stations F1 and E2 of synchrotron DORIS III in HASYLAB.

The back-reflection white beam synchrotron topographs provide fast and univocal possibility of detecting the additional unwanted polytypes in the epitaxial deposit. The roughness of the samples was determined by measuring the reflectometric curves and fitting the theoretical reflectometric curves computed using the REFSIM version 2.0 program based on the Parratt theory [18].

## 3. Results and discussion

Representative conventional topographs of the samples substrates obtained by means of conventional Lang and synchrotron topographic methods are shown in Fig. 1. The topographs enable resolving the individual dislocations, revealed as distinct dark lines and allow for evaluation of their density as being at the level  $10^3 \text{ cm}^{-2}$ . Some of the dislocations vanish in the particular topographs due to the extinction effect – the dependence of the contrast on the  $\cos(\mathbf{g}\mathbf{b})$  value (where  $\mathbf{g}$  is the diffraction vector and  $\mathbf{b}$  is the Burgers vector of the dislocation). Usually, the back-reflection topographs in symmetric transmission reflection do not reveal the dislocations with the Burgers vector parallel to the hexagonal axis  $\mathbf{c}$  [ $00 \cdot 1$ ], which provide much more extended (stronger) images in the back reflection topographs. The transmission topographs in Fig. 1a–c, taken in  $101$  – and  $-101$  reflections reveal some characteristic long segments of dislocations inclined at a very small angle to the surface sample, which are the basal plane dislocations, with the Burgers vector in the  $(00 \cdot 1)$  plane. In some regions of the topograph 1c one can notice some darker fields stretched between the dislocation lines, which correspond to stacking faults. Some weak contrasts of the stacking faults outcropping the surface were observed also in highly asymmetric reflections in the white beam back-reflection projection topographs – *e.g.* in Fig. 2. Usually these topographs reveal the dislocations in the form of dark dots or commas.

It was possible to confirm the identification of some dislocations, mainly the screw-type ones, by comparing the multi-crystal topographical images obtained in the monochromatic beam with numerically simulated images. The monochromatic beam topographs, which are highly analogous to the double-crystal topographs, provide the images of dislocations in the form of characteristic rosettes sometimes exhibiting an additional tail of the interference fringes coming from the dislocation core, as it was firstly observed and explained by Bubakova, Bedyńska and Sourek [19].

It was also possible to improve the simulated monochromatic beam images and the correspondence to the experimental ones by adding a large number of images each one with randomly introduced imperfections, analogously with finding the incoherent solution in the statistical dynamical theories. The procedure is justified by the expected presence of the small, almost incoherent inclusions, and the relatively large extension of the experimental images, requiring the assumption of a *non*-coherent beam. The exemplary experimental images and simulations including the presence of randomly distributed defects are shown in Fig. 3.

The topographic investigations performed after the deposition of the epitaxial layers in the samples with  $8^\circ$  and  $4^\circ$  off-cut confirmed the continuation of the dislocations in the epitaxial deposit, as it may in particular be observed in Fig. 4, especially in the monochromatic beam topograph (Fig. 4 b). Some representative screw dislocations with the contrast analogous to that in Fig. 3

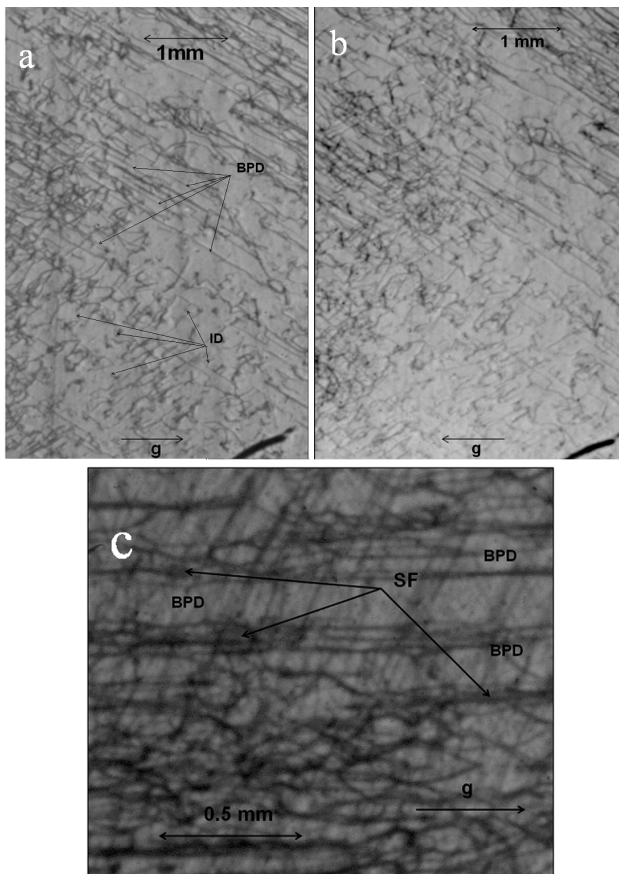


Fig. 1. Representative Lang topographs in 101 – a) and -101 – b) reflections of Mo  $K_{\alpha 1}$  radiation of 4H SiC substrates with  $4^\circ$  off-cut, and – c) enlarged fragment of Lang-topograph in 201 reflection of Mo $K_{\alpha 1}$  radiation with basal plane dislocations (long lines) and stacking-faults (darker regions split between parallel parts of long dislocation lines). “*SF*” denotes the representative stacking faults, “*BPD*” the basal plane dislocation, and “*ID*” the representative dislocations inclined to the surface at a relatively large angle. One can notice a significant difference in contrast of some dislocations between topographs 1a and 1b.

were marked on the subsequent stripes of the “zebra pattern”. The continuation of dislocations is confirmed also by Bragg-case section topographs (Fig. 4 c and d). Part of this topograph located further from the line of the intersection of incident beam with the surface should reveal mainly the dislocations and inclusions located in the substrate which do not distinctly differ from the dislocation in the epitaxial deposit.

We did not observe the formation either of new dislocations or of other extended defects in the epitaxial layers at all three growth rates. However, we found a distinct difference of the surface roughness in the layers deposited at different growth rates: the roughness increased with increasing applied growth rate, as may be seen from the fitted theoretical rocking curves in Fig. 5.

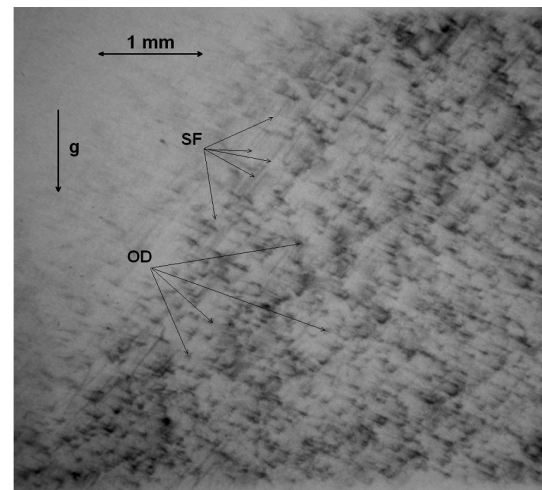


Fig. 2. Bragg-case synchrotron white beam projection topograph in an significantly asymmetric reflection with a large penetration depth revealing some dislocation outcropping the substrate – denoted as “*OD*” and images of basal plane dislocations with stacking faults, forming elongated weaker contrasts and marked representatively as “*SF*”.

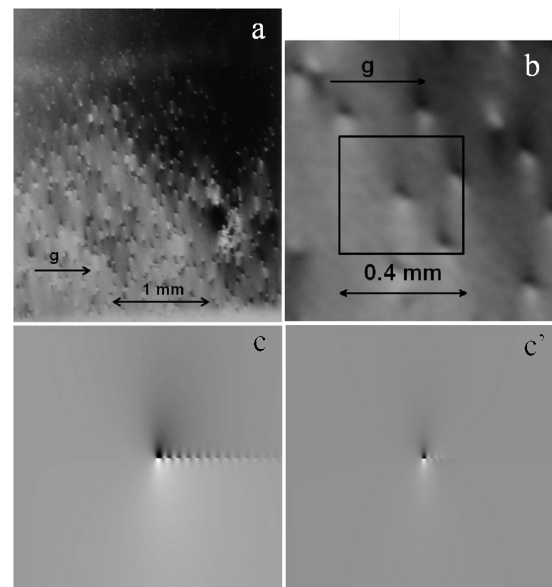


Fig. 3. a)-Monochromatic beam image revealing well resolved dislocations outcrops, many of them are screw-type, almost perpendicular to the surface and b) its enlarged fragment revealing some outcrops of the screw dislocations; c) – the simulation of the outcrop of the screw dislocation in the ideal crystal, taking into account the finite divergence of the incident beam and c') the improved simulation of the screw dislocation obtained by adding a large number of images each one with randomly introduced imperfections which significantly improves the correspondence of the simulated image to the experimental images. The dimensions of the theoretical images are equal to  $400 \mu\text{m}$ .

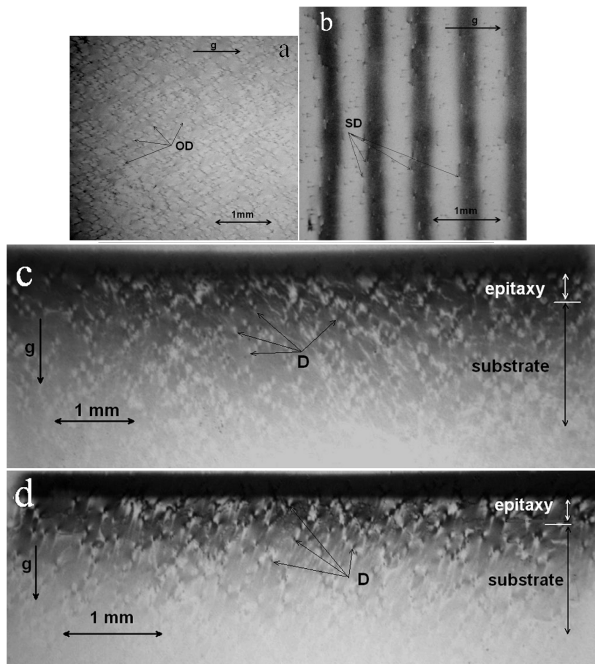


Fig. 4. a) Bragg-case projection topograph of a representative epitaxial deposit revealing mainly the dislocations outcropping the surface, b) the monochromatic beam “zebra-pattern” revealing the dislocations outcrops - some representative outcrops of the screw dislocations providing similar images as in Figs. 3b) are marked by “SD”, c) and d) the Bragg-case section topographs, differing in the structure factor, of the same sample revealing mainly the dislocations in the substrate (the defects from the  $5\ \mu\text{m}$  epitaxial layer are visible in the narrow upper part of the topographs close to the strong black stripe corresponding to the reflection of the slit from the surface) - the representative contrasts corresponding to dislocations are marked “D”.

The roughness values evaluated in the case of the epitaxial layers on the  $8^\circ$  substrates, were on much lower level of 1.2 nm, and the difference between the layers deposited with different growth rates was not distinct.

The topographic investigation performed after the epitaxial deposition indicated, however, a certain modification of dislocation structure inside the substrate. This modification consisted in less regular character of the dislocations arrangement, which often exhibited a certain curvature. Also some observed additional darker or white-dark contrasts seem to suggest formation of individual precipitates along the dislocation lines.

The applied conditions were not suitable to obtain the single polytype 4H SiC epitaxial deposit for the substrates with  $0^\circ$  off-cut, and the obtained layer contained a large amount of differently distributed other polytypes, especially the 3C one. An interesting phenomenon was observed in the case of the layer deposited at  $11\ \mu\text{m}/\text{h}$  growth rate, when the 3C and 15R polytypes formed islands of relatively large dimensions reaching single hundreds of microns or even single millimeters. These islands

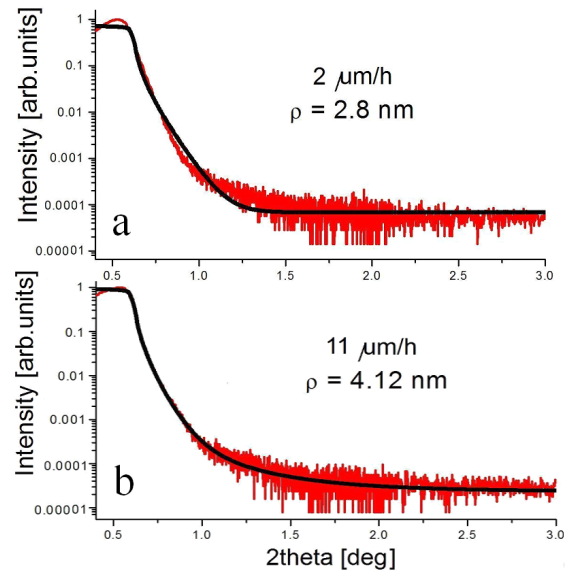


Fig. 5. The specular reflectometric curves for the grown epitaxial 4H silicon carbide layers deposited with rates of  $2\ \mu\text{m}/\text{h}$  - a) and  $11\ \mu\text{m}/\text{h}$  - b) on the substrates with  $4^\circ$  off-cut with fitted theoretical curves computed with REFSIM program. Surface roughness (marked as  $\rho$ ) for the substrate was close to 1.8 nm.

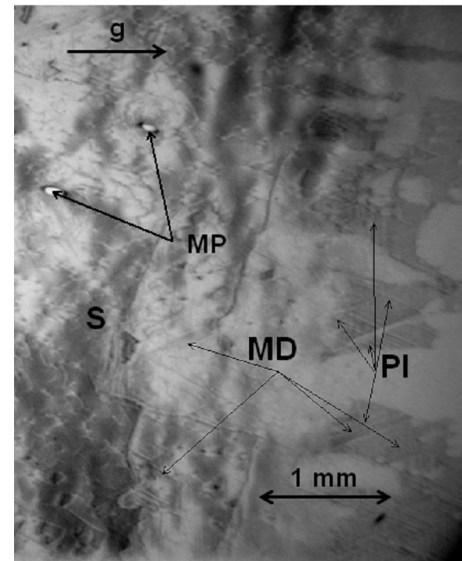


Fig. 6. Bragg-case projection topograph of the epitaxial layer grown with the highest rate  $11\ \mu\text{m}/\text{h}$  on  $0^\circ$  off-cut substrate revealing some large islands of other SiC polytype (most probably of 3C type) denoted by “PI” (in Fig. 6 the symbol is “PI”) containing misfit dislocations denoted representatively as “MD”. The upper-left half of the topograph reveal the image of the substrate denoted as “S” and the two micro-pipes present in the substrate are marked “MP”.

contained low density of misfit dislocations and other new created defects as may be seen in Fig. 6.

The investigation of some other samples confirmed the possibility of obtaining a single polytype 4H SiC homoepitaxial layers at higher growth temperature on the substrates with 0° off-cut, but the investigated layers often exhibited significant irregularities of the surface.

#### 4. Conclusions

The topographic investigations performed after the deposition of the epitaxial layers grown on 8° and 4° off-cut (00·1) 4H-SiC substrates confirmed the continuation of the dislocations in the epitaxial deposit. We did not observe either any formation of new dislocations or any other extended defects in the epitaxial layers grown in all three growth rates. On the contrary we found a distinct difference in the surface roughness of the layers deposited at different growth rates, which was increasing with the applied growth rate.

The results confirm the possibility of obtaining the epitaxial SiC layers with low concentration of defects at the substrates with 4° off-cut, but obtaining low surface roughness requires lower growth rates.

Applied conditions were not suitable to obtain the single polytype 4H SiC epitaxial deposit for the substrates with 0° off-cut and the obtained layer contained a large amount of other silicon carbide polytypes, especially 3C and 15R.

An interesting phenomenon was observed in the case of the layer deposited at 11  $\mu\text{m}/\text{h}$ , when other polytypes formed islands of relatively large dimensions reaching hundreds of microns or even single millimeters. These islands contained isolated misfit dislocations and other new defects.

#### Acknowledgements

The present work was supported by the grant of Ministry of Science and High Education, N N 505 379737 while the synchrotron investigations were supported by the EC 20100001 HASYLAB project.

#### References

[1] V.A. Dimitriev, High-Temperature Electronics in Europe – *Report International Technology Research Institute*, Chapter 2 (2000), [http://itri2.org/ttec/the\\_e/report/](http://itri2.org/ttec/the_e/report/).

- [2] Y. Abe, J. Komiyama, S. Suzuki, H. Nakanishi, *J. Cryst. Growth* **283**, 41 (2005).
- [3] T. Kimoto, A. Itoh, H. Matsunami, *Phys. Stat. Sol. b* **202**, 247 (1997).
- [4] H. Matsunami, T. Kimoto, *Mat. Sci. Eng.: R: Reports* **20**, 125 (1997).
- [5] K. Wada, T. Kimoto, K. Nishizawa, H. Matsunami, *J. Cryst. Growth* **291**, 1407 (2006).
- [6] W. Chen, K.-Y. Lee, M. Capano, *J. Cryst. Growth* **297**, 265 (2007).
- [7] K. Kojima, S. Nishizawa, S. Kuroda, H. Okamura, K. Arai, *J. Cryst. Growth* **275**, e549 (2005).
- [8] R. Myers, Y. Shiskin, O. Kordina, S.E. Sadow, *J. Cryst. Growth* **285**, 486 (2005).
- [9] H. Fujiwara, K. Danno, T. Kimoto, T. Tojo, H. Matsunami, *J. Cryst. Growth* **281**, 188 (2005).
- [10] B.E. Landini, G.R. Brandes, *Appl. Phys. Lett.* **74**, 2632 (1999).
- [11] D. Nakamura, I. Gunjishima, S. Yamaguchi, T. Ito, A. Okamoto, H. Kondo, S. Onda, K. Takatori, *Nature* **430**, 7003 (2004).
- [12] M. Benamara, X. Zhang, M. Skowronski, P. Ruterana, G. Nouet, J.J. Sumakeris, M.J. Paisley, M.J. O'Loughlin, *Appl. Phys. Lett.* **86**, 021905 (2005).
- [13] H. Tsuchida, I. Kaamata, M. Nagano, *J. Cryst. Growth* **310**, 757 (2008).
- [14] X. Zheng, M. Skowronski, K.X. Liu, R.E. Stahlbush, J.J. Sumakeris, M.J. Paisley, M.J.O. Loughin, *J. Appl. Phys.* **102**, 093520 (2007).
- [15] S.W. Huh, H.J. Chung, M. Benamara, M. Skowronski, J.J. Sumakeris, M.J. Paisley, *J. Appl. Phys.* **96**, 4637 (2004).
- [16] K. Kościewicz, W. Strupiński, W. Wierzchowski, K. Wieteska, A. Olszyna, *Mater. Sci. Forum* **645-648**, 251 (2009).
- [17] K. Mazur, W. Wierzchowski, K. Wieteska, W. Hofman, H. Sakowska, K. Kościewicz, W. Strupiński, W. Graeff, *Acta Phys. Pol. A* **117**, 272 (2009).
- [18] L.G. Parrat, *Phys. Rev.* **95**, 359 (1954).
- [19] T. Bedyńska, R. Bubakova, Z. Sourek, *Phys. Stat. Sol. (a)* **36**, 509 (1976).